Pharmacogn. Mag.
A multifaceted peer reviewed journal in the field of Pharmacognosy and Natural Products
www.phcog.com | www.phcog.net

ORIGINAL ARTICLE

Cell Cycle Arrest and Apoptosis in Human Liver Cancer Cell Line and A549 Cell Lines by Turbiconol– A Novel Sterol Isolated from *Turbinaria conoides*

Kala K. Jacob[1,2], K. J. Prashob Peter[1], S. Muraleedharan Nair[1], N. Chandramohanakumar[1,2]

[1]Department of Chemical Oceanography, School of Marine Sciences, Cochin University of Science and Technology, [2]Inter University Center for Development of Marine Biotechnology, Cochin University of Science and Technology, Cochin, Kerala, India

Submitted: 19-12-2018 Revised: 31-01-2019 Published: 26-08-2019

ABSTRACT

Background: *Turbinaria conoides*, a brown seaweed, is a rich source of oxygenated fucosterols which are capable of suppressing the proliferation of cancer cells. Their specific therapeutically significant biological activity is directly related to the unique structural features of the molecule. This study specifically focuses on extracting unconventional sterol molecules (side chain extension) from this seaweed which can be used as a lead molecule to evolve therapeutical agents. **Materials and Methods:** To isolate unconventional sterol molecule, for structural elucidation and bioactivity study, sufficient amount of *T. conoides* was collected from Mandapam, an unique biodiverse environment along the Southeast coast of India. State-of-the-art methods available for the purification and characterization of molecule (High-resolution fast-atom bombardment mass spectrometry, ultraviolet-visible spectroscopy, attenuated total reflection–fourier transform infra-red, One-dimensional nuclear magnetic resonance, and two-dimensional nuclear magnetic resonance) were put in. *In vitro* bioassays (3-(4,5-Dimethylthiazol-2-yl)-2,5-Diphenyltetrazolium bromide, double staining, and flowcytometry) were carried out against A549 and human liver cancer cell line (HepG2) malignant cells to assess the cytostatic potential. Data were statistically validated. **Results:** A unique unconventional sterol molecule (Turbiconol) with ethyl and methyl group at C-27 was isolated. This molecule induced apoptosis in A549 and HepG2. However, cell cycle assessment revealed G0/G1 cell cycle arrest in Hep G2 and G2/M checkpoint was responsible for the suppression of A549 cell line. **Conclusion:** A novel unconventional compound, turbiconol, is reported in this study. *In vitro* results highlight the potential of this molecule in developing therapeutical combination which can be used for novel treatment methods.

Key words: Cytotoxicity, seaweeds, sterol, turbiconol, *Turbinaria conoides*

SUMMARY

- *Turbinaria conoides*, brown seaweed, was collected and treated with popular organic solvents to isolate bioactive sterols. Extracts were subjected to conventional chromatographic purification and fine purification by preparative high-performance liquid chromatography. Pure compound was characterized with the aid of multiple spectroscopic tools such as ultraviolet-visible spectroscopy, attenuated total reflection–fourier transform infra-red, nuclear magnetic resonance (H-nuclear magnetic resonance, C13-nuclear magnetic resonance, distortionless enhancement by polarization transfer, correlation spectroscopy, heteronuclear single-quantum coherence, heteronuclear multiple bond correlation), and mass spectroscopy (fast-atom bombardment mass spectrometry and Gas chromatography-mass spectrometry). Based on the data, a novel sterol molecule with unique structural features was isolated and named it as turbiconol. Cytotoxicity, antiproliferative mechanism, and influence on cell cycle of A549 and human liver cancer cell line by turbiconol were further studied. These assessments revealed the potential of molecule to suppress lung and liver cancer along with mode of action. Even though apoptosis was induced in both cell lines, the mechanism of cell cycle arrest was different. In A549, G2/M cell cycle arrest was observed, whereas G0/G1 cell cycle arrest was induced in the human liver cancer cell line. The results highlight the promising potential of turbiconol in developing drug combinations to suppress the activity of malignant cells.

Abbreviations used: DNMR: One-dimensional nuclear magnetic resonance spectroscopy; DNMR: Two-dimensional nuclear magnetic resonance spectroscopy; AO: Acridine orange; ATR-FTIR: Attenuated total reflection-fourier transform infrared; A549: Adenocarcinomic human alveolar basal epithelial cells; CDK: Cyclin-dependent kinase; DEPT: Distortionless enhancement by polarization transfer; DMEM/F2: Dulbecco's Modified Eagle Medium/nutrient mixture F-12; EB: Ethidium bromide; ED_{50}: Effective dose-50; GC-MS: Gas chromatography-mass spectrometry; G0: A phase where the cell has left the cycle and has stopped dividing; G1: The G1 checkpoint control mechanism ensures that everything is ready for DNA synthesis; G2: During the gap between DNA synthesis and mitosis, the cell will continue to grow. The G2 checkpoint control mechanism ensures that everything is ready to enter the M (mitosis) phase and divide; HepG2: Human liver cancer cell line; HMBC: Heteronuclear multiple bond correlation; HPLC: High-performance liquid chromatography; HR-FAB-MS: High-resolution fast-atom bombardment mass spectrometry; HSQC: Heteronuclear single-quantum coherence; M: Cell growth stops at this stage and cellular energy is focused on the orderly division into two daughter cells; MTT: 3-(4,5-Dimethylthiazol-2-yl)-2,5-Diphenyltetrazolium Bromide; NCCS: National Centre for Cell Science; PBS: Phosphate-buffered saline; UV-VIS: Ultraviolet-visible spectroscopy.

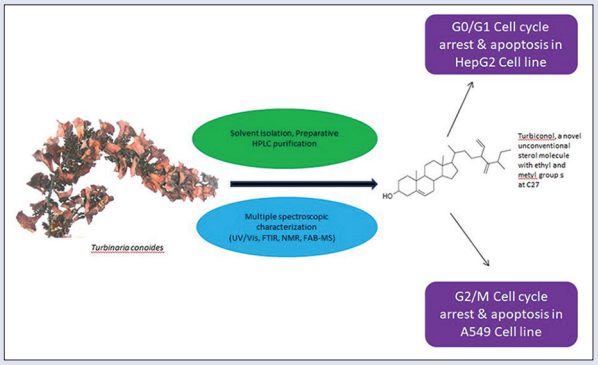

Correspondence:

Dr. Kala K. Jacob,
Inter University Center for Development of Marine Biotechnology, Cochin University of Science and Technology, Cochin - 682 016, Kerala, India.
E-mail: kalajacob@cusat.ac.in
DOI: 10.4103/pm.pm_643_18

Access this article online
Website: www.phcog.com
Quick Response Code:

Cite this article as: Jacob KK, Peter KJ, Nair SM, Chandramohanakumar N. Cell cycle arrest and apoptosis in human liver cancer cell line and A549 cell lines by Turbiconol– A novel sterol isolated from *Turbinaria conoides*. Phcog Mag 2019;15:S189-96.

INTRODUCTION

Sterols and its derivatives belong to the most systematically studied secondary metabolite with respect to their biological activity.[1,2] Significant biological potency showcased by these molecules is assigned to their unique side chain stereochemistry.[3] Among side chain-modified sterols, side chain-extended sterols (unconventional sterols) are very rare in nature and their presence has been reported only in *Aplysina fistulari* and *Jaspis stellifera*. Aplysterol from *A. fistulari*, stelliferasterol, and isostelliferasterol discovered by Theobald *et al.* and dehydroaply-sterol from *J. stellifera* are the sterols so far reported in this class of sterol molecules.[4,5] Further, only available data regarding their bioactivity is the inhibitory effect shown by aplysterol on human DNA topoisomerase II-α. Due to limited data on the bioactivities of unconventional sterols and considering the wide range of bioactivity spectrum shown by side chain-modified sterols, detailed investigation of these molecules is required to assess their therapeutical potential.[6] This study focuses on the isolation and characterization of side chain-extended sterols from *T. conoides* and its anti-cancerous potency against A549 and human liver cancer cell line (HepG2) human cancer cell lines.

Due to the metastatic nature of lung and liver cancer, their early treatment and curing is very vital. However, suppressing the proliferation of these cells without causing side effects is a challenge.[7-9] A detailed understanding of mechanism by which unconventional sterol molecule shows inhibitive effects against *in vitro* cell models will aid in developing cancer chemopreventive agents with reduced side effects. In this regard, A549 and HepG2 are excellent cell models for lung and liver cancer, which aids in delineating cellular mechanisms and gene modulations triggered by the test compound to suppress the cancer cells.[10-12]

In this investigation for novel pharmaceutically important unconventional sterol molecule, we applied semi-preparative high-performance liquid chromatography (HPLC) coupled with bioassay to expedite the isolation of cytotoxic sterol from prefractionated extracts of *T. conoides*. Side chain extension in the sterol molecule was validated with aid of multiple spectroscopic tools such as fourier transform infrared (FTIR), mass spectroscopy, and one-dimensional and two-dimensional nuclear magnetic resonance (NMR) spectroscopy. Cell viability, double staining, and flowcytometry studies were performed to assess the cytotoxic potential and mechanism of action against lung and liver cancer.

MATERIALS AND METHODS

Sampling, processing, and analytical techniques

Approximately 50 kg of *T conoides*, a brown seaweed belonging to Sargassacea family, was collected from Mandapam coastline (latitude 9° 45'N and longitude 79°E), during premonsoon. Prior to preservation samples were washed with sea water followed by distilled water and stored in deep freezer at −20°C until the extraction process. *T. conoides* is an abundant seaweed present in the coast of the Indian subcontinent and is a storehouse of unique secondary metabolites with potential bioactivity[13-15] and biocompatibility.[16,17]

Semi-quantitative preparative HPLC (Shimadzu LC 20AT), equipped with an SCL-10Avp controller and a SPD-10Avp detector was used for the purification of turbiconol. Conventional methods were used for the melting point analysis. Specific rotation of the sample (0.1% turbiconol dissolved in HPLC grade $CHCl_3$) was evaluated at 25°C using optics manual polarimeter.[18]

Absorbance maxima of the compound were measured using Specord 200 plus ultraviolet-visible spectroscopy (UV-Vis) spectrophotometer. 1 mg of the isolated compounds was dissolved in chloroform and absorbances were measured from 200 to 750 nm. Chloroform was used as reagent blank.

Nature of the functional groups and double bond characteristics were assessed using attenuated total reflection-FTIR (ATR-FTIR) (Perkin Elmer, Spectrum 100) by recording the vibrational characteristics of the molecule in the mid-infrared region. Prior to FTIR analysis, N_2 gas was purged on the surface of the instrument to remove moisture. High-resolution (4 cm^{-1}) ATR transmission mode spectra for sterol were acquired over the mid-infrared region (4000–600 cm^{-1}).[18]

Bruker 400 NMR spectrometer operating at 300 K was used to collect NMR data (δH, δC, correlation spectroscopy [COSY], distortionless enhancement by polarization transfer [DEPT], heteronuclear single-quantum coherence, and heteronuclear multiple bond correlation [HMBC]). For NMR analysis, 5 mg of sterol was dissolved in $CDCl_3$.[18]

Fast-atom bombardment mass spectrometry (FAB-MS) (Joel SX 102/DA-6000 mass spectrometer) was used to obtain the exact mass of turbiconol. Sterol sample (0.1 mg) in 100 µL HPLC grade methanol was used for the analysis. The quasimolecular ions (M + H) + spectrum were recorded at room temperature. The spectrum is obtained at resolution of 1000 amu. Mass spectra patterns were obtained with gas chromatography-MS (GC-MS) (Perkin Elmer, Clarus 680-Clarus 600T) system. Sterol 1 mg was dissolved in 1 mL ethyl acetate and 1 µL was injected to GCMS equipped with nonpolar HP ultra-double fused silica capillary column.[18] Novelty of the identified sterol was confirmed with the aid of SciFinder®.

Cell culture

Liver hepatocellular cells (HepG2) and human lung adenocarcinoma (A549) cell lines were purchased from the National Centre for Cell Science, Pune, India. Dulbecco's modified Eagles media (DMEM/F2) was used and culture conditions were maintained at humidified 5% CO_2 and 37°C of optimum temperature until a 70%–80% confluence was reached. 10% Foetal Bovine Serum and antibiotics such as penicillin G (100 µL/mL), streptomycin (100 mg/mL), and amphotericin (250 ng/mL) were supplemented in culturing media. Trypsinization was performed with 0.5% (W/V) trypsin (0.25%, Invitrogen, USA) and ethylenediaminetetraacetic acid for 3 min at 37°C, only after attaining appropriate confluence. Appropriate cell suspensions obtained were used for further experimental procedures.

Procedure

To access the cytotoxic potential of turbiconol against lung and liver cancer, A549 and HepG2 human cell lines at a density of 2 × 105 cell/mL seeded in a 96-well microtiter plate was used. These cells were further incubated for 24 h at 37°C in a 5% CO_2 atmosphere to ensure the complete cell adhesion. Cell adhesion to substrate was further verified using microscope. The plates were further used to access the antiproliferates mechanism and cell cytostatic activities.

Cytotoxicity of turbiconol

The changes in the cell viability were evaluated by thiazolyl blue tetrazolium bromide (3-(4,5-Dimethylthiazol-2-yl)-2,5-Diphenyltetrazolium Bromide [MTT] assay). Prior to turbiconol exposure to access cell viability well plates were seeded with 1000 trypsinized A549 and Hep G2 cell lines. After 24 h, these cells were treated with different concentration of turbiconol (6.5, 12.5, 25, 50, and 100 µg/mL) followed by 24 h incubation at 37°C in a 5% CO_2 atmosphere. Negative controls (untreated cells) were included in all experimental runs. After turbiconol exposure for 24 h, media were carefully decanted from the plate and formazan product formed was dissolved in 200 µL dimethyl sulfoxide to evaluate the absorbance at 570 nm using microplate reader.[19] The data are reported as mean ± standard error (*n* test = 3). Morphological changes of cells after

exposure to turbiconol, were studied by inverted microscope Olympus CKX4.[19,20] Experimental replications performed for morphological change is $n = 2$.

Antiproliferative mechanism of turbiconol

Optical fluorescence microscopy which utilizes the differential absorption of fluorescent DNA-binding dyes (such as EB/AO staining) was used to study chromatin condensation and fragmentation of nuclei along with cell death mechanism in HepG2 and A549 human cell lines.[21] In this assay, as there is no further cell binding step, apoptosis index and the integrity of cell membrane can be evaluated at the same time without articrafts. Apoptotic and necrotic cells can be quantified simultaneously in real time, making it a format suitable for high throughput screening of drugs. DNA-binding dyes acridine orange (AO) and ethidium bromide (EB) were purchased from Sigma Aldrich, USA. Both viable and non-viable cells assimilate AO and upon intercalation with DNA emit green fluorescence.[22] However, EB is taken up by non-viable cells only and emit red fluorescence when intercalated with DNA. This differential absorption of dyes by viable and non-viable cells along with variation in the emitted fluorescence was effectively used to determine exact mechanism of cell death.[22]

Cell lines after incubation with test samples, i.e., ED_{50} of turbiconol, were stained with AO (100 µg/mL) and EB (100 µg/mL) at room temperature for 10 min, after washing with cold phosphate-buffered saline (PBS) and before their visualization in a blue filter of fluorescence microscope (Olympus CKX41 with Optika Pro5 camera). The cells were divided into four categories based on the observation. They are living cells with normal green nucleus, early apoptotic cells are having bright green nucleus with condensed or fragmented chromatin, late apoptotic are observed as orange-stained nuclei with chromatin condensation, and finally, necrotic cells have uniformly orange-stained cell nuclei. Experimental replications performed for double staining assay is $n = 2$.

Influence of turbiconol on the cell cycle

Possible cell cycle effects caused by turbiconol exposure were assessed by direct measurement of DNA synthesis using Muse® Cell Cycle Assay Kit. For performing fluorescence activated sorting analysis, cell lines treated with samples were incubated at 37°C for 24 h. After incubation, the cells were collected by trypsinization and washed twice with 1 × PBS. These concentrated cells were thoroughly washed with PBS. After washing by PBS, 1 mL ice cold ethanol (Merck) was used to fix these cells and was incubated overnight at −20°C. Again an additional washing of ethanol-fixed cells was carried out using PBS. These cells were then uniformly mixed with muse cell cycle reagent (Millipore, USA) and incubated for 30 min in the dark. After incubation, these cells were analyzed using flow cytometer (Muse™ Cell analyser, USA). A set of untreated cells were used as control.[23,24] Experimental replications performed for cell cycle analysis is $n = 2$.

ED_{50} calculation

ED_{50}plus V1.0 software (online free excel add in software) was used to calculate ED_{50} values from MTT assay.

RESULTS

White amorphous solid: m. p. 156°C–158°C; $(\alpha)^{25}$D-28 (c 0.1 $CHCl_3$); UV-Vis λ_{max} 243 nm; Appendix A: IR (neat) υ_{max} 3664 cm^{-1}, υ_{max} 1451 cm^{-1} and υ_{max} 1044 cm^{-1} [Figure S1]; EI-MS 428 (4), 410 (10), 367 (29), 349 (18), 271 (90), 255 (30), 161 (28), 109 (49), 95 (86), 43 (100) [Figure S2]; ^{1}H and ^{13}C NMR data, see Table 1 [Figure S3-S9]; and positive ion HR-FAB-MS, m/z 453.63 $(M + H)^+$ (calculated 453.76) was obtained in 0.085% yield from *T. conoides*.

Characterization of sterol

The novel secondary metabolite, turbiconol (1) with 7°C unsaturation and molecular formula $C_{32}H_{52}O$ [Figure 1] was isolated as white amorphous solid from *T. conoides*.In the HR-FAB-MS, the $(M + H)^+$ molecular ion peak was developed at m/z 453.63.The spectroscopic data from ^{13}C and DEPT analysis of compound showed that it has 32 carbons [Table 1], which included four quarternary carbons, ten

Table 1: Nuclear magnetic resonance spectral data of turbiconol (δ in ppm, *J* in Hz)

Serial number	DEPT	δ_C	δ_H
1	CH_2	37.273	1.08 m, 1.83 m
2	CH_2	31.73	1.83 m
3	CH	71.816	3.53 tdd *J*=11.0, 5.3, 4.1 Hz
4	CH_2	42.38	2.28 m, 2.23 m
5	C	140.78	
6	CH	121.689	5.36 dt *J*=5.3, 1.9 Hz
7	CH_2	31.94	1.49 m, 1.95 m
8	CH	31.923	1.96 m
9	CH	50.149	0.92 m
10	C	36.52	
11	CH_2	21.091	1.49 m
12	CH_2	34.801	1.57 m, 1.60 m
13	C	36.52	
14	CH	56.779	1.07 m
15	CH_2	24.284	1.57 m
16	CH_2	29.113	1.02 m
17	CH	55.855	1.09 m
18	CH_3	11.857	0.68 s
19	CH_3	19.935	1.01 m
20	CH	35.928	1.38 m
21	CH_3	17.559	0.88 s
22	CH_2	39.78	1.15 m, 2.00 m
23	CH_2	28.171	1.83 m
24	CH	36.146	1.72 m
241	CH	142.579	5.81 ddd *J*=17.5, 10.9, 5.5 Hz
242	CH_2	112.89	5.16 m
25	C	142.50	
26	CH_2	112.854	5.21 m
27	CH	36.087	1.73 m
27a	CH_2	28.219	1.41 m
27b	CH_3	18.790	0.93 m
27a'	CH_3	16.462	0.91 m

DEPT: Distortionless enhancement by polarization transfer

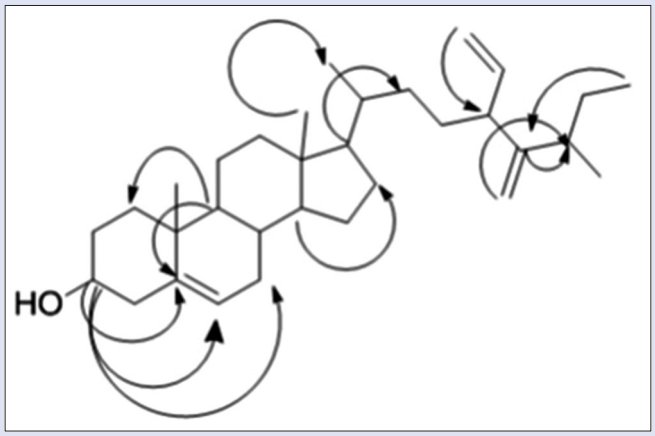

Figure 1: Heteronuclear multiple bond correlation correlations of turbiconol

methine carbons, 13 methylene carbons, and five methyl carbons. The UV spectrum of compound revealed the presence of endocyclic double bound (λ_{max} 243 nm).[18] The IR data of 1 revealed the presence of hydroxy group (υ_{max} 3664 cm^{-1}), CH_2 attached to olefinic carbon (υ_{max} 1451 cm^{-1}) and a highly polarized OH group vibration at C_3 along with the existence of C_5=C_6 double bond and formation of intramolecular hydrogen bond between C_3-OH and C_5=C_6 double bond (υ_{max} 1044 cm^{-1}).[25] The EI-MS of turbiconol gave significant fragment ion peaks at m/z 410 $(M-43)^+$, 367 $(M-85)^+$, 271 $(M-SC-2H)^+$, and 255 $(M-SC-OH)^+$ characteristic of sterol moieties.[26,27]

The ^{1}H NMR spectrum [Table 1] showed signals due to two tertiary methyl groups (δ_H 0.68, 3H, s, H_3-18; δ_H 0.88 3H, s, H_3-19), a C-27 ethyl, methyl sterol side chain (δ_H 1.73), three olefinic protons (δ 5.80 (ddd, *J* = 17.5, 10.9, 5.5 Hz, 2H), 5.35 (dt, *J* = 5.3, 1.9 Hz, 2H), 5.24–5.09 (m, 2H) and a methine proton on carbon bearing a hydroxy group (δ_H 3.53, 1H, m, H-3). ^{1}H NMR coupling information in the ^{1}H-^{1}H COSY spectrum of 1 enabled identification of H_2-1/H_2-2/H-3/H_2-4, H-6/H_2-7/H-8/H-9/H_2-11/H_2-12, H-8/H-14/H_2-15/H_2-16/H-17/H-20/H_2-22/H_2-23/H-24, H-20/H_3-21, H-24/H-24a/H_2-24b, H-25/H-26, H-25/H_2-27a/$_{H3}$-27a', and H-25/H_3-27b [Table 1]. These data with the key HMBC correlations between protons and quaternary carbon such as H_3-27b/C-25; H_2-24b/C-24; H_2-26/C27; H-17/C21, H_1-5, H_2-6, H_2-7/C-3; H_2-1, H-5/C-9 [Table 1], permitted the elucidation of the main carbon skeleton of 1. Novelty of turbiconol was confirmed by SciFinder® software (CAS, Columbus, U.S.A).

Cytotoxicity of turbiconol

Along with morphology alterations, MTT viability assay was used to quantify the HepG2 and A549 cell viability changes [Figures 2 and 3] to five different doses of turbiconol (6.25, 12.5, 25, 50, and 100 μg/mL) at 24 h. After 24 h exposure, significant changes in the cell viability rate was observed in all cell models studied using MTT and as the concentration of turbiconol increased, the percentage of live cell was reduced considerably. Cell viability was found to exhibit a dose-dependent pattern with compound treatment [Figure 4]. ED_{50} values for turbiconol against A549 is 66.353 μg/mL. At lowest concentration of 6.5 μg/mL, turbiconol induced a cell death of 13.59% in lung cancer cell line. Significant cell death was observed with 65.02% for turbiconol, at the higher concentration range (100 μg). Whereas, against HepG2 ED_{50} is 60.98 μg/mL. Turbiconol, at 6.5 μg/mL concentration induced only 18.37% cell death. However, activity of sterol increased by almost 10% when concentration was increased to 12.5 from 6.5 μg/mL. At 50 μg/mL concentration of turbiconol, only 50.21% cells were viable.

Morphology of the cells exposed with turbiconol was evaluated in order to endorse the data obtained by MTT assay. Images of the morphology of cell confirmed that turbiconol has significant cytotoxic response in HepG2 and A549 cell lines after 24 h and exposure.[28-32]

Antiproliferative mechanism of turbiconol

Double staining assay was performed to assess the cytostatic mechanism operating in HepG2 and A549 cells exposed to turbiconol. After 24 h and exposure of HepG2 cell lines with turbiconol, cell nuclei were observed as orange in color [Figure 5]. Whereas, A549 cell nuclei were bright green in color [Figure 6] indicating apoptosis-induced cell death.[33]

Influence of turbiconol on cell cycle

Flow cytometry was used to measure the turbiconol interaction with cell cycle in HepG2 and A549 cells exposed to turbiconol. Exposure of HepG2 cell lines to ED_{50} concentration of turbiconol for 24 h caused an increase in the cell population in G0/G1 cell cycle 13.3% [Figure 7]. This was correlated to decreased number of cells in G2/M phase, 24.0%–8.7%. Whereas, for A549 cells exposed to turbiconol for 24 h G2/M cell cycle arrest (2.6%) at G2/M phase was observed and corresponding decrease in G0/G1 and S phases [Figure 8]. After 24 h, there was an elevation in the number of cells in the G0/G1 phase of the cell cycle treated with turbiconol.

DISCUSSION

This work intended to study the effect of turbiconol, an unconventional sterol molecule with ethyl and methyl group at C 27, on HepG2 and A549 cell line, in order to assess their future potential as chemotherapeutic agent for treating liver and lung cancer.

Morphological alterations in cells along with MTT viability assay clearly validated that turbiconol induced drug dosage response in both cell lines. ED_{50} value of turbiconol 60.914 μg/mL against HepG2 and 66.79 μg/mL against A549 deduced from MTT assay clearly demonstrate

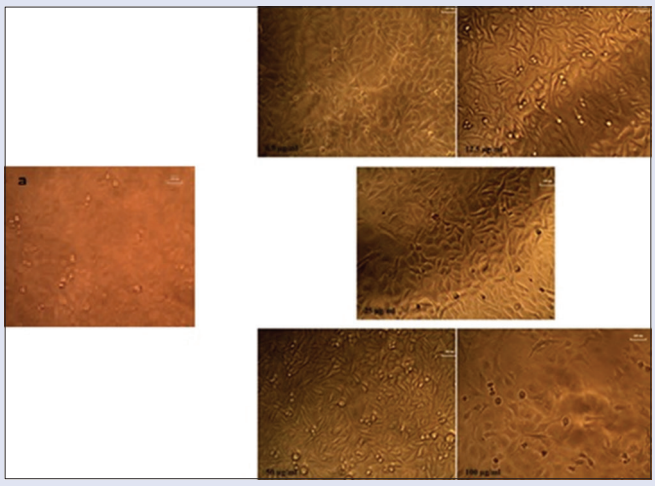

Figure 2: Phase contrast image of control cells (a) of human liver cancer cell line and changes in morphology when subjected to varying concentration turbiconol. Data represent representative image from experimental replication of *n* = 2

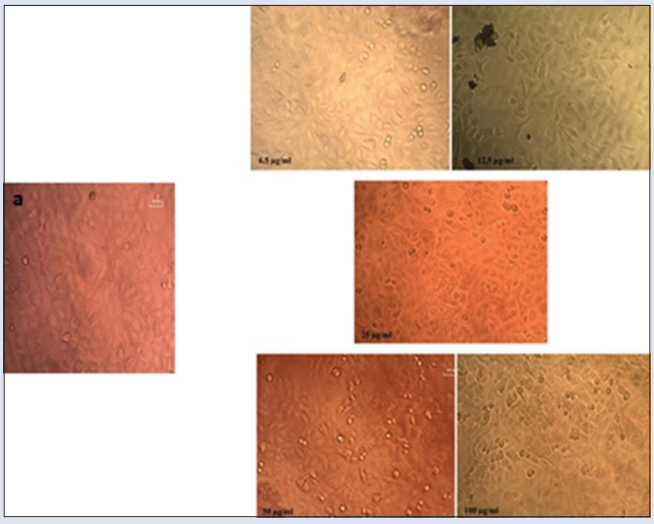

Figure 3: Phase contrast image control cells (a) of A549 cell line and changes in morphology when subjected to varying concentration of turbiconol. Data represent representative image from experimental replication of *n* = 2

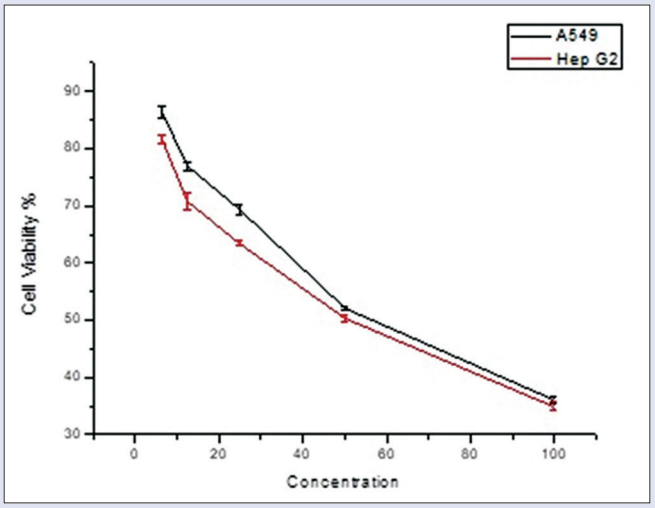

Figure 4: Graphical representations of cytotoxicity results. Cytotoxicity of turbiconol against human liver cancer cell line and A549 cell line by 3-(4,5-Dimethylthiazol-2-yl)-2,5-Diphenyltetrazolium Bromide assay. Data represent the mean ± standard error of triplicate experiments

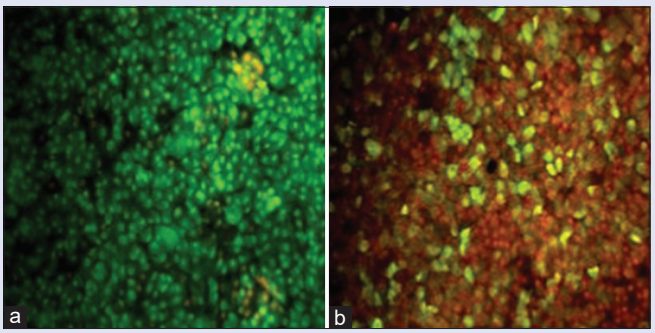

Figure 5: Detection of antiproliferative mechanism (apoptosis/necrosis) treated with acridine orange and ethidium bromide double staining (a) Untreated human liver cancer cell line control cell lines showing intact cells with green fluorescent nuclei (b) human liver cancer cell line cells treated with turbiconol. Data represent representative image from experimental replication of $n = 2$

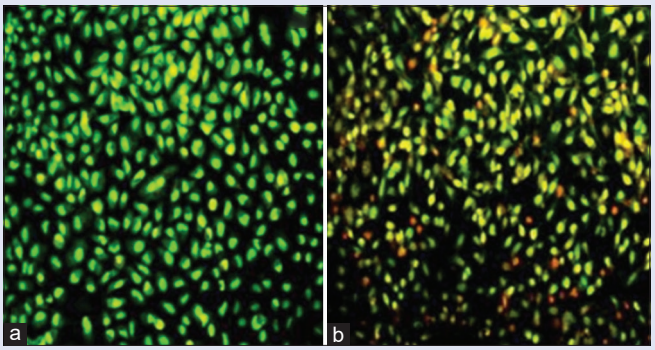

Figure 6: Detection of antiproliferative mechanism (apoptosis/necrosis) treated with acridine orange and ethidium bromide double staining (a) Untreated A549 control cell lines showing intact cells with green fluorescent nuclei (b) A549 cells treated with turbiconol. Data represent representative image from experimental replication of $n = 2$

moderate cytotoxic activity against these malignant cells. MTT results clearly indicated a significant loss of cell organelle integrity following exposure to turbiconol, which can be correlated to cell death. Loss of cell adhesion, shrinkage in cytoplasmic area, rounding up of cells, and nuclear condensation observed when dosed with turbiconol are marker for apoptotic cell death.[29-32] Expression of Caspase-9 activating receptors on the cell surface might be tempering by turbiconol dosage. Cytotoxic mechanism definitely depends nature of the cells, hence differential morphological response of HepG2 and A549 could be attributed to cell type.[21,22] It has been witnessed in various *in vivo* studies that sterol structure is a major factor that influences the suppression of malignant cells.[33-35]

Cells which perceived nucleus in bright green after double staining tracks a normal cell cycle [Figures 5 and 6]. Hep G2 cells when dosed with the turbiconol, nuclei were observed as orange color [Figure 5]. Moreover, these cells suffered extensive chromatin condensation or fragmentation. These features are consistent toward late apoptotic pathway of cell death in Hep G2[11,36] whereas, nucleus of A549 cell after 24 h and exposure to turbiconol consisted of condensed/fragment chromatin and nucleus appeared yellow-green in color. These observations predict early apoptotic pathway initiated by turbiconol. Cells which show normal cell death pattern and in case of early apoptotic with intact cell membranes are stained only by AO dye and results in green fluorescing spectra bound to DNA. Whereas, DNA fragments of apoptotic bodies allowed EB dye bond and exhibit an orange-red fluorescence, resulting from the late apoptotic or along with dead cells.[21]

Cells still with intact membranes but have started to undergo DNA cleavage interacts with AO stain and emits yellow-green fluorescence predominantly, a direct consequence of early apoptosis. Presence of bright green patches or fragments observed in A549 clearly highlights the perinuclear chromatin condensation. However, initiation of late apoptosis by sterol molecules is also inferred from the scattered emission of orange-red fluorescence.[21] Hep G2 cells on the other hand when dosed with the same turbiconol, nuclei were observed as orange. Further, these Hep G2 cells suffered extensive chromatin condensation or fragmentation. These features are consistent toward a late apoptotic pathway of cell death in Hep G2, as necrotic cells have uniformly orange to red nuclei with a condensed structure.[21]

The rates of cell proliferation and apoptosis are major controlling factors influencing the tumor growth.[37] Both phyto and phycosterols are effective apoptosis (programmed cell death) stimulants. Major mechanisms involved in the activation of apoptosis by sterols are membrane structure alteration, membrane fluidity, modulation of membrane-bound enzyme activity, signal transduction pathways and membrane integrity.[38] However, exact mechanisms are still elusive. Sterols are easily incorporated into the membranes due to their closely related structural similarities to cholesterol (an integral lipid component of biological membranes). However, assimilation of sterols by tumor cells alters the concentration of two phospholipids, i.e., sphingomyelin and phosphatidylcholine, which are involved in signal transduction pathways, thereby inducing apoptosis in malignant cells.[39-41] Further, proper fluidity balance is vital for the membrane functioning. Sterols are effective in altering the composition of lipid membranes and thereby influencing their fluidity and suppressing the progression of tumor growth.[42] For example, liver membrane fluidity of rats is altered by feeding them with supplements incorporated with 5% sterols for 21 days.[43]

Finally, differential influence of turbiconol on the cell cycle of HepG2 and A549 following 24 h and exposure was observed. While comparing population percentage in the different phases of HepG2 and A549 cells after 24 h and exposure to turbiconol, noteworthy changes were noticed. Studies have shown the cell cycle halt in cancer cells leads accumulation

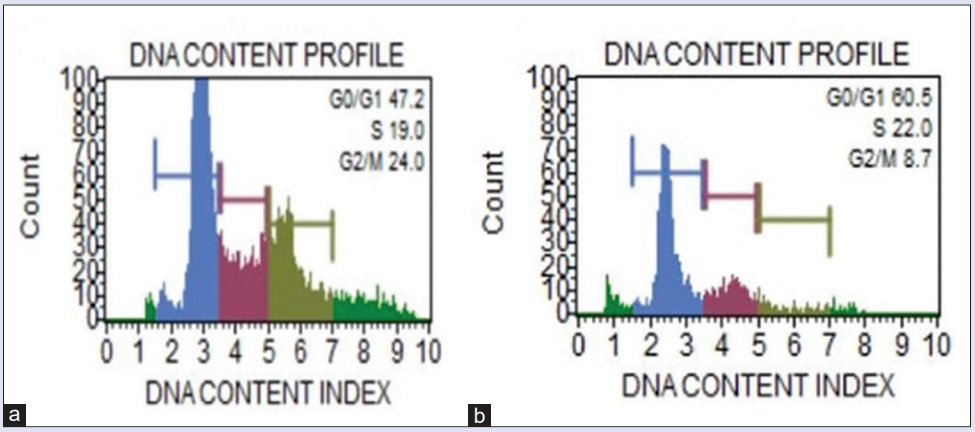

Figure 7: Flow cytometry cell cycle analysis using propidium iodide DNA staining. DNA content index of human liver cancer cell line (a) control cells (b) treated with turbiconol. Data represent representative graph from experimental replication of $n = 2$

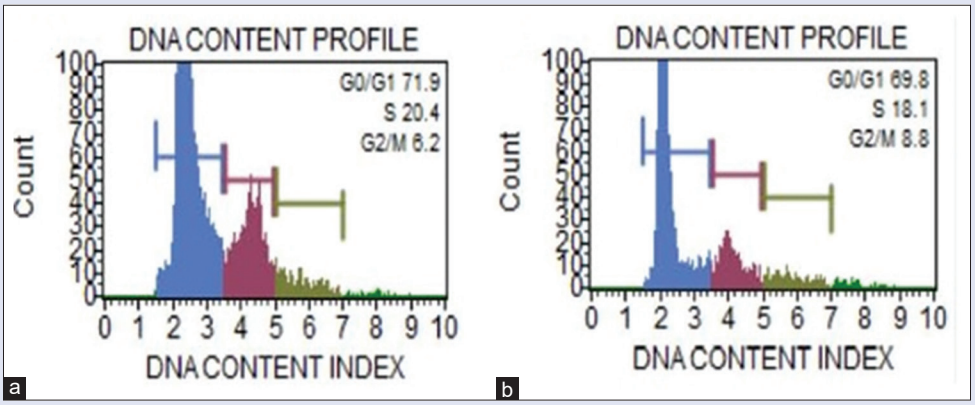

Figure 8: Flow cytometry cell cycle analysis using propidium iodide DNA staining. DNA content index of A549 cell line (a) control cells (b) treated with turbiconol. Data represent representative graph from experimental replication of $n = 2$

of cells with damaged DNA, means the growth inhibition in malignant cells.[44] Therefore, the alleviated HepG2 cell population in G0/G1 and A549 cell population in G2/M phases after 24 h highlights DNA damage prompted by turbiconol exposure, which might be leading to genotoxicity similar to what has been revealed for phytosterols in various cytotoxic studies.[45-47] The potential of anticancer compounds to participate in cell cycle to induce G1, S, or G2/M phase arrest with relation to their selectivity.[48-50] Many researchers have observed the downregulation of CDK2 found with cyclin E and CDK inhibitors, when treated with cancer suppressing compounds in normal progression of G1 to S phase.[51] Cell arrest at G2/M phase is also suggested by various researchers as major pathway for the initiation of apoptosis by phytosterols. G2/M cell cycle arrest results mainly from inappropriate cdc2 activation.[52] G2/M phase cell cycle arrest was observed in A549 cell lines when treated with turbiconol.

These observations suggest turbiconol, a novel side chain-extended sterol, isolated from *T. conoides* has the potential to induce early and late apoptosis in A549 and HepG2 cell lines. Since G2/M cell cycle arrest is used in combination with chemotherapy and radiation treatment methods, results of this study are of particular importance in cancer treatment.[52] G2/M phase cell cycle arrest induced by turbiconol in A549 cell line highlights its potential in developing therapeutic combinations to sensitize cells toward chemotherapy and radiation treatment methods for curing lung cancer.

CONCLUSION

An unconventional sterol structure with ethyl and methyl group at C27 for turbiconol was confirmed by the aid of multiple spectroscopic studies. Antiproliferative potential of turbiconol isolated from *T. conoides* against Hep G2 and A549 cancer cell lines are reveled using multiple cytotoxicity assays (MTT and Morphology). Double staining results confirmed the potential of sterol molecule to induce early and also late apoptotic events on cancer cells under investigation. The impact of test compound on cell cycle is vital while evaluating the therapeutical activity of compounds, as it provides a better insight into the interactions occurring at molecular level. Here, evaluation of cell cycle by flow cytometry strongly support apoptosis induced antiproliferative potential of turbiconol. Against Hep G2, turbiconol selectively induced apoptosis and arrest in G0/G1 cell cycle phase. Whereas, cell cycle halt in G2/M checkpoint was noticed in A549 cell lines when treated with turbiconol. Hence, these results advocate sterols in dietary inclusion and in drug combination for developing cell cycle and cell division targets for limiting cancer cell proliferation.

Acknowledgements

We are thankful to Biogenix Research Center for cytotoxic studies.

Financial support and sponsorship

The financial grant received from the Government of Kerala to establish new center, Inter University Center for Development of Marine Biotechnology is acknowledged.

Conflicts of interest

There are no conflicts of interest.

REFERENCES

1. Khanavi M, Gheidarloo R, Sadati N, Ardekani MR, Nabavi SM, Tavajohi S, *et al.* Cytotoxicity of fucosterol containing fraction of marine algae against breast and colon carcinoma cell line. Pharmacogn Mag 2012;8:60-4.
2. Saeidnia S, Gohari AR, Shahverdi AR, Permeh P, Nasiri M, Mollazadeh K, *et al.* Biological activity of two red algae, *Gracilaria salicornia* and *Hypnea flagelliformis* from Persian gulf. Pharmacogn Res 2009;1:428-30.
3. Kim JA, Son JH, Song SB, Yang SY, Kim YH. Sterols isolated from seeds of *Panax ginseng* and their antiinflammatory activities. Pharmacogn Mag 2013;9:182-5.
4. Ferriol P, Marante FJ, Martin IB, Rodríguez JJ, Alonso RG, Benkovics AG, *et al.* Identification and quantification, by NMR and LC-MS, of sterols isolated from the marine sponge *Aplysina aerophoba*. Rec Nat Prod 2018;12:470-9.
5. Theobald N, Wells RJ, Djerassi C. Minor and trace sterols in marine invertebrates. 8. Isolation, structure elucidation and partial synthesis of two novel sterols-stelliferasterol and isostelliferasterol. J Am Chem Soc 1978;100:7677-84.
6. Lira NS, Monte-Neto RL, Marchi JG, Lins AC, Tavares JF, Silva MS, *et al.* Aplysfistularine: A novel dibromotyrosine derivative isolated from *Aplysina fistularis*. Quim Nova 2012;35:2189-93.
7. Sikdar S, Mukherjee A, Khuda-Bukhsh AR. Anti-lung cancer potential of pure esteric-glycoside condurangogenin A against nonsmall-cell lung cancer cells *in vitro* via p21/p53 mediated cell cycle modulation and DNA damage-induced apoptosis. Pharmacogn Mag 2015;11:S73-85.
8. Bosch FX, Ribes J, Díaz M, Cléries R. Primary liver cancer: Worldwide incidence and trends. Gastroenterology 2004;127:S5-S16.
9. Bach PB, Kelley MJ, Tate RC, McCrory DC. Screening for lung cancer: A review of the current literature. Chest 2003;123:72S-82S.
10. McCormick C, Freshney RI. Activity of growth factors in the IL-6 group in the differentiation of human lung adenocarcinoma. Br J Cancer 2000;82:881-90.
11. Herrema H, Czajkowska D, Théard D, van der Wouden JM, Kalicharan D, Zolghadr B, *et al.* Rho kinase, myosin-II, and p42/44 MAPK control extracellular matrix-mediated apical bile canalicular lumen morphogenesis in HepG2 cells. Mol Biol Cell 2006;17:3291-303.
12. Abreu RM, Ferreira IC, Calhelha RC, Lima RT, Vasconcelos MH, Adega F, *et al.* Anti-hepatocellular carcinoma activity using human HepG2 cells and hepatotoxicity of 6-substituted methyl 3-aminothieno[3,2-b] pyridine-2-carboxylate derivatives: *In vitro* evaluation, cell cycle analysis and QSAR studies. Eur J Med Chem 2011;46:5800-6.
13. Sheu JH, Wang GH, Sung PJ, Duh CY. New cytotoxic oxygenated fucosterols from the brown alga *Turbinaria conoides*. J Nat Prod 1999;62:224-7.
14. Kala KJ, Prashob Peter KJ, Chandramohanakumar N. Cyto-toxic potential of fucosterol isolated from *Turbinaria conoides* against Dalton's lymphoma ascites. Int J Pharmacogn Phytochem Res 2015;7:1217-21.
15. Kala KJ, Prashob Peter KJ, Chandramohanakumar N. Analysis of antimicrobial potential of silver nanoparticles synthesized by fucoidan isolated from *Turbinaria conoides*. Int J Pharmacogn Phytochem Res 2016;8:1959-63.
16. Prashob PK, Kala KJ, Chandramohanakumar N. Cytotoxic potential of humic acid synthesized silver nano plates against Dalton's lymphoma ascites. Int J Toxi Pharma Res 2016;8:425-9.
17. Thomas A, Peter PK, Chandramohanakumar N. A profiling of anti-tumour potential of sterols in the mangrove fern *Acrostichum aureum*. Int J Pharma Phyto Res 2016;8:1828-32.
18. Goad J, Akihisa T. Analysis of Sterols. London: Blackie Academic and Professional Press; 1997.
19. Loveland BE, Johns TG, Mackay IR, Vaillant F, Wang ZX, Hertzog PJ. Validation of the MTT dye assay for enumeration of cells in proliferative and antiproliferative assays. Biochem Int 1992;27:501-10.
20. Sylvester PW. Optimization of the tetrazolium dye (MTT) colorimetric assay for cellular growth and viability. Methods Mol Biol 2011;716:157-68.
21. Ribble D, Goldstein NB, Norris DA, Shellman YG. A simple technique for quantifying apoptosis in 96-well plates. BMC Biotechnol 2005;5:12.
22. Gherghi IC, Girousi ST, Voulgaropoulos AN, Tzimou-Tsitouridou R. Study of interactions between DNA-ethidium bromide (EB) and DNA-acridine orange (AO), in solution, using hanging mercury drop electrode (HMDE). Talanta 2003;61:103-12.
23. Pozarowski P, Darzynkiewicz Z. Analysis of cell cycle by flow cytometry. In Checkpoint Controls and Cancer. New York City: Humana Press; 2004. p. 301-11.
24. Darzynkiewicz Z, Huang X, Zhao H. Analysis of cellular DNA content by flow cytometry. Curr Protoc Immunol 2017;119:5.7.1-5.7.20.
25. Levchuk YN, Khalimonova IN. Infrared absorption in C-OH stretching vibration bands of unsaturated sterols. Appl Spectrosc 1969;11:818-20.
26. Cho JH, Djerassi C. Minor and trace sterols from marine invertebrates. 58. Stereostructure and synthesis of new sponge sterols jaspisterol and isojaspisterol. J Org Chem 1987;52:4517-21.
27. Kobayashi M, Tomioka A, Mitsuhashi H. Marine sterols. VIII. Isolation and structure of sarcosterol, a new sterol with a delta17(20)-double bond from the soft coral *Sarcophyton glaucum*. Steroids 1979;34:273-93.
28. Plumb JA, Milroy R, Kaye SB. Effects of the pH dependence of 3-(4,5-dimethylthiazol-2-yl)-2,5-diphenyl-tetrazolium bromide-formazan absorption on chemosensitivity determined by a novel tetrazolium-based assay. Cancer Res 1989;49:4435-40.
29. Earnshaw WC, Martins LM, Kaufmann SH. Mammalian caspases: Structure, activation, substrates, and functions during apoptosis. Annu Rev Biochem 1999;68:383-424.
30. Los M, Wesselborg S, Schulze-Osthoff K. The role of caspases in development, immunity, and apoptotic signal transduction: Lessons from knockout mice. Immunity 1999;10:629-39.
31. Rashedi I, Panigrahi S, Ezzati P, Ghavami S, Los M. Autoimmunity and apoptosis – Therapeutic implications. Curr Med Chem 2007;14:3139-51.
32. Vijayarathna S, Sasidharan S. Cytotoxicity of methanol extracts of *Elaeis guineensis* on MCF-7 and vero cell lines. Asian Pac J Trop Biomed 2012;2:826-9.
33. Xu X, London E. The effect of sterol structure on membrane lipid domains reveals how cholesterol can induce lipid domain formation. Biochemistry 2000;39:843-9.
34. Rueda A, Zubía E, Ortega MJ, Salvá J. Structure and cytotoxicity of new polyhydroxylated sterols from the Caribbean gorgonian *Plexaurella grisea*. Steroids 2001;66:897-904.
35. Roh EM, Jin Q, Jin HG, Shin JE, Choi EJ, Moon YH, *et al.* Structural implication in cytotoxic effects of sterols from *Sellaginella tamariscina*. Arch Pharm Res 2010;33:1347-53.
36. Liu K, Liu PC, Liu R, Wu X. Dual AO/EB staining to detect apoptosis in osteosarcoma cells compared with flow cytometry. Med Sci Monit Basic Res 2015;21:15-20.
37. Elmore S. Apoptosis: A review of programmed cell death. Toxicol Pathol 2007;35:495-516.
38. Awad AB, Chinnam M, Fink CS, Bradford PG. Beta-sitosterol activates fas signaling in human breast cancer cells. Phytomedicine 2007;14:747-54.
39. Pörn MI, Slotte JP. Localization of cholesterol in sphingomyelinase-treated fibroblasts. Biochem J 1995;308(Pt 1):269-74.
40. Slotte JP. Sphingomyelin-cholesterol interactions in biological and model membranes. Chem Phys Lipids 1999;102:13-27.
41. Awad AB, Fink CS. Phytosterols as anticancer dietary components: Evidence and mechanism of action. J Nutr 2000;130:2127-30.
42. Spector AA, Yorek MA. Membrane lipid composition and cellular function. J Lipid Res 1985;26:1015-35.
43. Leikin AI, Brenner RR. Fatty acid desaturase activities are modulated by phytosterol incorporation in microsomes. Biochim Biophys Acta 1989;1005:187-91.
44. Kim S, Ryu DY. Silver nanoparticle-induced oxidative stress, genotoxicity and apoptosis in cultured cells and animal tissues. J Appl Toxicol 2013;33:78-89.
45. Suárez Y, Fernández C, Ledo B, Martín M, Gómez-Coronado D, Lasunción MA. Sterol stringency of proliferation and cell cycle progression in human cells. Biochim Biophys Acta 2005;1734:203-13.
46. Wu TH, Yang RL, Xie LP, Wang HZ, Chen L, Zhang S, *et al.* Inhibition of cell growth and induction of G1-phase cell cycle arrest in hepatoma cells by steroid extract from meretrix meretrix. Cancer Lett 2006;232:199-205.
47. Zhao YY, Shen X, Chao X, Ho CC, Cheng XL, Zhang Y, *et al.* Ergosta-4,6,8 (14),22-tetraen-3-one induces G2/M cell cycle arrest and apoptosis in human hepatocellular carcinoma HepG2 cells. Biochim Biophys Acta 2011;1810:384-90.
48. Gallagher BM Jr. Microtubule-stabilizing natural products as promising cancer therapeutics.

Curr Med Chem 2007;14:2959-67.

49. Boesze-Battaglia K, Brown A, Walker L, Besack D, Zekavat A, Wrenn S, *et al*. Cytolethal distending toxin-induced cell cycle arrest of lymphocytes is dependent upon recognition and binding to cholesterol. J Biol Chem 2009;284:10650-8.
50. Zhao G, Cui J, Zhang JG, Qin Q, Chen Q, Yin T, *et al*. SIRT1 RNAi knockdown induces apoptosis and senescence, inhibits invasion and enhances chemosensitivity in pancreatic cancer cells. Gene Ther 2011;18:920-8.
51. Guadagno TM, Newport JW. Cdk2 kinase is required for entry into mitosis as a positive regulator of Cdc2-cyclin B kinase activity. Cell 1996;84:73-82.
52. Awad AB, Burr AT, Fink CS. Effect of resveratrol and beta-sitosterol in combination on reactive oxygen species and prostaglandin release by PC-3 cells. Prostaglandins Leukot Essent Fatty Acids 2005;72:219-26.